Journal of Organometallic Chemistry 934 (2021) 121661

Contents lists available at ScienceDirect

Journal of Organometallic Chemistry

journal homepage: www.elsevier.com/locate/jorganchem

Synthesis, structure and catalytic activity of rare-earth metal amino complexes incorporating imino-functionalized indolyl ligand

Lu Yu[a], Fenhua Wang[b], Hui Wang[a], Shaoyin Wang[a], Yunjun Wu[a], Xiaoxia Gu[a,*]

[a] Institute of Synthesis and Application of Medical Materials, Department of Pharmacy, Wannan Medical College, Wuhu, Anhui 241002, PR China
[b] College of Biological and Chemical Engineering, Anhui Polytechnic University, Wuhu, Anhui 241000, PR China

ARTICLE INFO

Article history:
Received 19 July 2020
Revised 10 December 2020
Accepted 17 December 2020
Available online 20 December 2020

ABSTRACT

The reactions of the imino-functionalized indolyl ligand (H**L**, **L** = 3-(4-Me_2N-C_6H_4CH=N-CH_2CH_2)C_8H_5N) with the rare-earth metal amides $[(Me_3Si)_2N]_3RE(\mu\text{-Cl})Li(THF)_3$ producing different types of rare-earth metal amido complexes were investigated. The reactions of H**L** with 1 equiv. of $[(Me_3Si)_2N]_3RE(\mu\text{-Cl})Li(THF)_3$ generated a series of hetero-nuclear bimetallic rare-earth metal amino complexes $\{[\eta^1{:}\mu\text{-}\eta^2$-3-(4-$Me_2N$-$C_6H_4CH$=N-$CH_2CH_2$)$C_8H_5$]RE[$N(SiMe_3)_2$]$_2(\mu$-Cl)Li(THF)$\}$ (RE = Y(**1**), Sm(**2**), Gd(**3**), Er(**4**), Yb(**5**)). By extending the reaction time, only the reaction of H**L** with $[(Me_3Si)_2N]_3Gd(\mu\text{-Cl})Li(THF)_3$ gave an unexpected binuclear rare-earth metal complex $\{[(\mu\text{-}\eta^5{:}\eta^1){:}\eta^1{:}\eta^1$-3-[$(Me_2N)_2$-$C_{14}H_9$]-($NCH_2CH_2$-$C_8H_5N)_2$]$Gd_2$[$N(SiMe_3)_2$]$_3\}$ (**6**) incorporating a novel polycyclic ligand through C-C and C-N coupling. Treatment of H**L** with $[(Me_3Si)_2N]_3Sm(\mu\text{-Cl})Li(THF)_3$ in a 2:1 ratio generated the bis(indolyl) heteronuclear bimetallic rare-earth metal amino complex $\{(\eta^1{:}\eta^1$-[$\mu\text{-}\eta^2{:}\eta^1$-3-(4-$Me_2N$-$C_6H_4CH$=N-$CH_2CH_2$)$C_8H_5$]Li[$\mu\text{-}\eta^2{:}\eta^1$-3-(4-$Me_2N$-$C_6H_4CH$=N-$CH_2CH_2$)$C_8H_5$])Sm[$N(SiMe_3)_2$]$_2\}$ (**7**) in low yield probably due to accompanying with the formation of the complex **2**. The above results indicated that reaction conditions play important roles in the formation of different coordination modes of the imino-functionalized indolyl rare-earth metal amido complexes. All new complexes **1**–**7** are fully characterized including X-ray structural determination. The catalytic activity of complexes **1**-**7** for the addition of amines to carbodiimides was explored. The results showed that all complexes displayed an excellent activity towards the addition of amines to carbodiimides producing guanidine under solvent-free condition.

© 2020 Elsevier B.V. All rights reserved.

1. Introduction

Functionalized indolyl ligands are used widely in organometallic and coordination chemistry of rare-earth metals for their strong electron-donating indolyl ring and the precise tailoring of the metal coordination sphere, and enable the complexes to be used as homogeneous catalysis [1]. Various rare-earth metal complexes (alkyls, amides) stabilized by functionalized indolyl ligands have been synthesized and structurally characterized [2]. Moreover, these complexes have been found to be efficient catalysts or pre-catalysts for C–C [2c-d, 2e, 2g] C-N [2h] and C-P [2a-b, 2i] bond construction. Among these work, the reactions of different pyrrolyl-functionalized indoles with rare-earth metal amides $[(Me_3Si)_2N]_3RE(\mu\text{-Cl})Li(THF)_3$ generated different kinds of rare-earth metal amido complexes [2f-g]. The findings encouraged us to explore the reactivity of imino-functionalized indolyl ligand with rare-earth metal amides.

Many substituted guanidines have biologically and pharmaceutically activities [3], such as antimicrobial [4], anti-cancer agents [5]. They are also widely used as ligands in organometallic and coordination chemistry [6]. Meanwhile guanidine derivatives are used in many kinds of base-catalyzed reactions [7]. As a result, various methods have been explored for the synthesis of guanidines [8], among them, metal catalytic addition of amines to carbodiimides is a straightforward and atom-economic route to substituted guanidine [9]. Since Hou's group employed the half-sandwich lanthanide alkyl complexes as catalysts for this reaction [10a], the development of rare-earth metal catalysts for the transformation has attracted increasing attention [10]. Shen's group found ytterbium triflate to be efficient catalyst for the reaction under solvent-free condition [10c]. This finding aroused chemists' enthusiasm and many kinds of rare-earth metal complexes with different ancillary ligands had been found for this reaction under solvent-free condition subsequently, such as β-diketiminate [10d, 10f], N-heterocyclic carbene [10e], and bridged bis(amidate) [10g]. However, the draw-

* Corresponding author.
E-mail address: guxiaoxia@wnmc.edu.cn (X. Gu).

https://doi.org/10.1016/j.jorganchem.2020.121661
0022-328X/© 2020 Elsevier B.V. All rights reserved.

backs such as steric of ligands and the ionic radii of rare-earth metals in most cases remain to be solved. Thus, searching for new kinds of high efficiency catalysts to synthesis of substituted guanidine under solvent-free condition is still required.

We herein report the synthesis and structural characterization of new rare-earth metal amides supported by imino-functionalized indolyl ligand. The reaction of imino-functionalized indolyl ligand with rare-earth metal amides $[(Me_3Si)_2N]_3RE(\mu\text{-}Cl)Li(THF)_3$ obtained three kinds of rare-earth metal complexes under different conditions. The structures of new complexes **1**-**7** are elucidated by X-ray crystallography and spectrometry analysis. Their catalytic addition of arylamines to carbodiimides under solvent-free condition was examined.

2. Results and discussion

2.1. Ligand synthesis

The reaction of tryptamine with *p*-(*N, N*-dimethylamino) benzaldehyde in ethanol at room temperature gave 4-(((2-(1H-indol-3-yl)ethyl)imino)methyl)-*N, N*-dimethylaniline (H**L**) in high yield (Scheme 1).

2.2. Synthesis and characterization of the hetero-nuclear bimetallic rare-earth metal amino complexes

Treatments of $[(Me_3Si)_2N]_3RE(\mu\text{-}Cl)Li(THF)_3$ with 1 equiv. of 4-(((2-(1H-indol-3-yl)ethyl)imino)methyl)-*N,N*-dimethylaniline (H**L**) at 80 °C in toluene for 24 h generated a series of hetero-nuclear bimetallic rare-earth metal amido complexes$\{[\eta^1{:}\mu\text{-}\eta^2\text{-}3\text{-}(4\text{-}Me_2N\text{-}C_6H_4CH{=}N\text{-}CH_2CH_2)C_8H_5]RE[N(SiMe_3)_2]_2(\mu\text{-}Cl)Li(THF)\}$ (RE = Y(**1**), Sm(**2**), Gd(**3**), Er(**4**), Yb(**5**)) in 23~41% yields (Scheme 2, route a).

Complexes **1**-**5** were readily crystallized from hexane at room temperature, X-ray diffraction studies revealed that all the complexes shared similar structural features. As shown in Fig. 1, the rare-earth metal ion adopted a distorted tetrahedral geometry consisting of one η^1-bonded N atom of the indolyl ring, two $N(SiMe_3)_2$ groups, and an additional chloride ligand that also bridged the lithium ion. The latter was ligated to the α- and β-carbon of indolyl ring in an η^2 fashion. Further coordination with the imine N

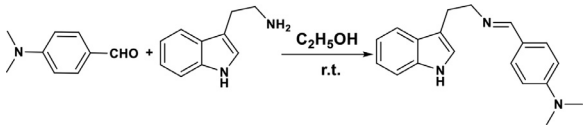

Scheme 1. Preparation of the ligand H**L**.

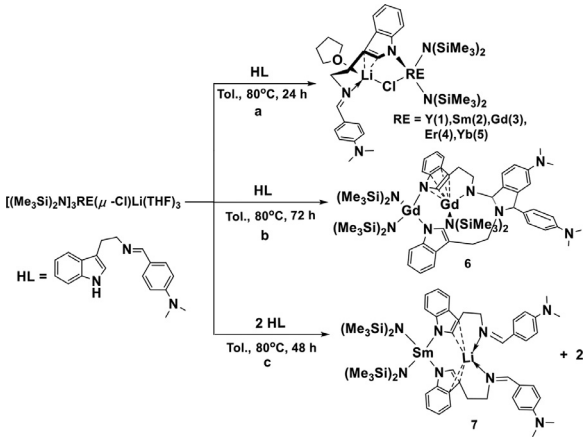

Scheme 2. Preparation of complexes **1**-**7**.

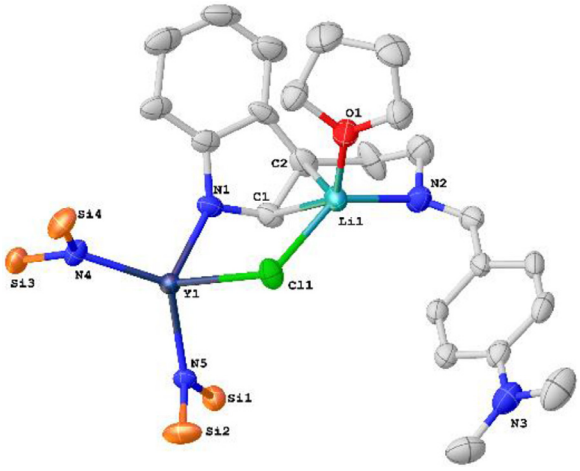

Fig. 1. Representative molecular structure of complex **1**. Hydrogen atoms and the CH_3 of $N(SiMe_3)_2$ group were omitted for clarity.

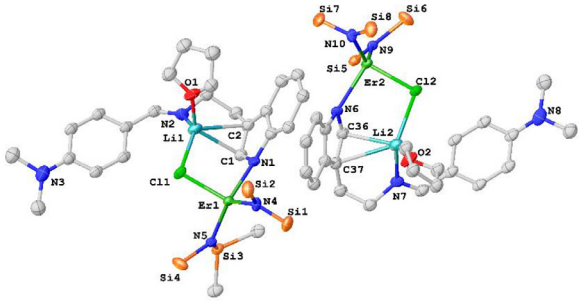

Fig. 2. Representative molecular structure of complex **4**. Hydrogen atoms and CH_3 of $N(SiMe_3)_2$ group were omitted for clarity.

atom from the pendant arm and one molecular of THF completed its coordination sphere, leading to a distorted triangular pyramid geometry. Interestingly, the crystal lattice of complex **4** contains two independent molecules in which the arrangement of ligands on the lithium ions led to two enantiomers. The representative molecular structure of complexes **1** and **4** are shown in Figs. 1,2. The selected bond lengths and angles of complexes **1**-**5** were listed in Table 1.

The average distances between a rare-earth metal ion and an N1 atom of an indolyl ring, gradually increased from 2.248(5) in **5** to 2.352(6) Å in **2**, are well consistent with the trend of ionic radii of the corresponding lanthanide elements. For comparison, the bond lengths of Y-N1 (2.271(4) Å) and Er-N1 (2.324(9) Å) are closed to those of hetero-nuclear bimetallic complexes $\{[(Me_3Si)_2N]_2RE[\eta^1{:}\mu\text{-}\eta^2\text{-}3\text{-}(2\text{-}(N\text{-}CH_3)C_4H_3NCH{=}N\text{-}CH_2CH_2)\text{-}C_8H_5](\mu\text{-}Cl)Li(THF)\}$ (RE = Y (2.280(3) Å), Er (2.301(6)) Å) [2j]. However, the distances between a lithium ion and α-position (or β-position) carbon atom of an indolyl ring are distinctly longer than the reported hetero-nuclear bimetallic complexes [2g], which might be attributed to differences steric of ligand.

When the reaction time was prolonged to 72 h, the reaction of H**L** with 1 equiv. of $[(Me_3Si)_2N]_3Gd(\mu\text{-}Cl)Li(THF)_3$ generated the unexpected binuclear complex **6** $\{[(\mu\text{-}\eta^5{:}\eta^1){:}\eta^1{:}\eta^1\text{-}3\text{-}[(Me_2N)_2\text{-}C_{14}H_9]\text{-}(NCH_2CH_2\text{-}C_8H_5N)_2]Gd_2[N(SiMe_3)_2]_3\}$ (Scheme 3, route b, Fig. 3), which was isolated in 12% yield after crystallization from hexane. However, the similar result was not observed in the reaction of H**L** with other $[(Me_3Si)_2N]_3RE(\mu\text{-}Cl)Li(THF)_3$ under the same conditions.

As shown in Fig. 3, the crystal structure of complex **6** contained two Gd^{3+} ions that lie in distinct coordination sphere. One Gd^{3+} ion (Gd1), one indolyl ring ligated in an η^5 mode, the tertiary

Table 1
Selected bond lengths (Å) and angles (°) for complexes **1**-**5**.

	1	2	3	4	5
RE-N1	2.271(4)	2.352(6)	2.310(5)	2.324(9)	2.248(5)
RE-N4	2.211(3)	2.283(6)	2.248(4)	2.285(8)	2.178(5)
RE-N5	2.226(4)	2.265(5)	2.256(5)	2.295(8)	2.180(5)
RE-Cl	2.5932(14)	2.670(2)	2.6374(18)	2.407(4)	2.5542(18)
Cl-Li	2.368(9)	2.351(14)	2.353(12)	2.39(2)	2.374(13)
Li-C1	2.635(11)	2.622(17)	2.613(14)	2.40(2)	2.602(16)
Li-C2	2.635(12)	2.643(18)	2.632(15)	2.58(3)	2.637(17)
Li-O1	1.887(10)	1.921(16)	1.926(13)	1.86(2)	1.909(14)
Li-N2	2.029(10)	2.008(17)	2.001(13)	2.07(2)	2.031(14)
N1-RE-N4	112.37(14)	107.5(2)	112.73(19)	103.2(3)	112.2(2)
N4-RE-N5	121.52(14)	120.7(2)	120.50(19)	126.4(3)	121.8(2)
N1-RE-N5	108.42(16)	114.1(2)	108.0(2)	115.1(3)	108.3(2)
N4-RE-Cl	99.89 (10)	125.13(16)	99.57(13)	124.2(2)	100.03(14)
N5-RE-Cl	122.15 (11)	97.92(15)	123.83(14)	92.9(2)	121.59(16)
N1-RE-Cl	87.56(11)	87.11(17)	87.72(14)	90.0(2)	88.03(15)

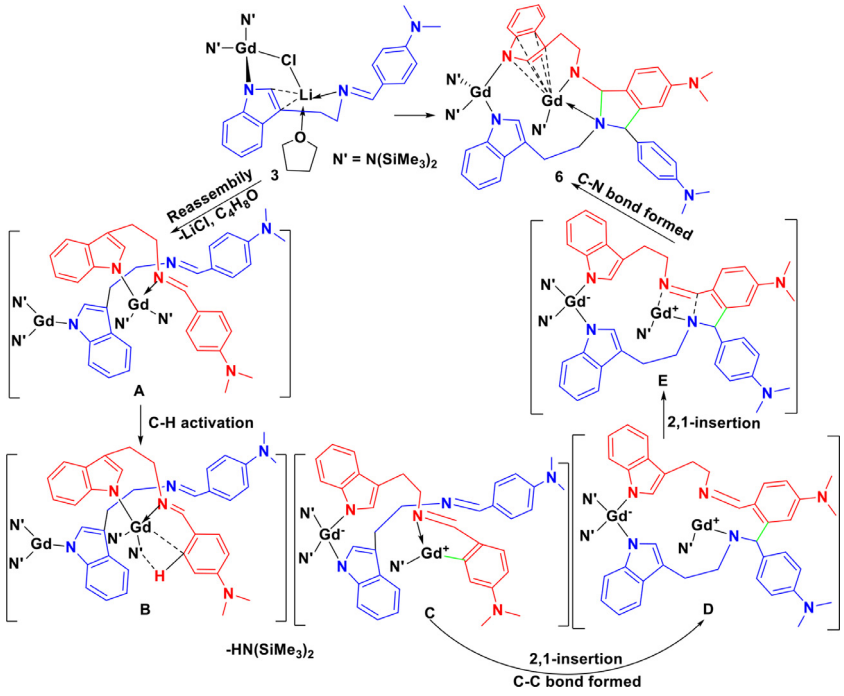

Scheme 3. Proposed pathway for the formation of complex **6.**

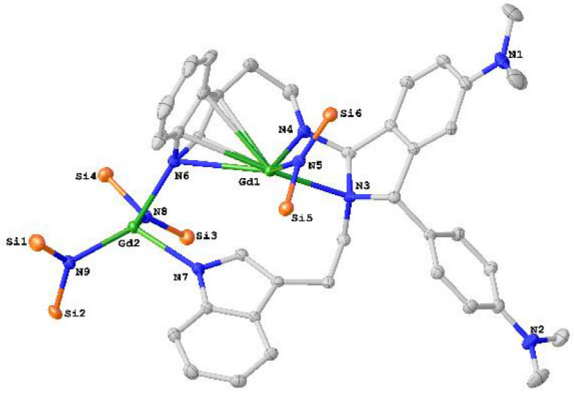

Fig. 3. Structure of complex **6**. Hydrogen atoms and the CH_3 of $N(SiMe_3)_2$ group were omitted for clarity.

amino N atom (N3) and the secondary amino N atom (N-4) in an η^1 mode respectively. The coordination from the pendent amido and $N(SiMe_3)_2$ group led to a distorted tetrahedral geometry on Gd1. For the other Gd^{3+} ion (Gd2) also possesses a distorted tetrahedral geometry consisting of two η^1-bonded indolyl rings via the N atoms, and two $N(SiMe_3)_2$ groups. The selected bond lengths and angles of complex **6** are listed in Table 2.

The formation of complex **6** included a C–H bond activation and C–C and C–N bonds forming steps. The activation of sp^2 C–H bond of pyridine [11], imidazole [12], indole [2j], or aromatic aldimines [13] by rare-earth metal alkyl or amido complexes was well documented. On the basis of these works, a possible pathway of the formation of complex **6** is proposed. The reaction was initiated by a ligand redistribution of two molecules of complex **3** (intermediate A), The intermediate **A** would go through a process involving the activation of the *ortho* sp^2 C–H bond of phenyl group in aldimine to form intermediate **B**. Then, the Gd1-C bond was formed, the indolyl ring subsequently changed its coordination centre from Gd1 to Gd2 to lead to Gd1 become cationic alkyl species (intermediate **C**). The step reaction was similar to the diastereodivergent annulations of aldimine with styrene via C–H activation [13]. Then, the resulted cationic Gd-phenyl-amido moiety then underwent a tandem insertion process to form C-C (intermediate **D**) [2j, 11b] and

Table 2
Selected bond lengths (Å) and angles (°) for complex **6.**

	Bond lengths (Å)		Angles (°)
Gd1-N3	2.676(4)	N3-Gd1-N4	57.06(13)
Gd1-N4	2.261(4)	N5-Gd1-N3	95.91(13)
Gd1-N5	2.328(4)	N5-Gd1-N6	121.94(14)
Gd1-N6	2.859(4)	N5-Gd1-C1	139.35(15)
Gd1-C1	2.803(5)	N5-Gd1-C2	118.29(16)
Gd1-C2	2.914(5)	N5-Gd1-C3	94.31(16)
Gd1-C3	2.995(5)	N5-Gd1-C4	96.43(15)
Gd1-C4	2.953(5)	N6-Gd2-N7	83.49(14)
Gd1-Ind[a]	2.905(5)		
Gd2-N7	2.371(4)	N6-Gd2-N8	102.98(15)
Gd2-N8	2.335(4)	N6-Gd2-N9	126.12(16)
Gd2-N9	2.306(4)	N7-Gd2-N8	105.71(15)
Gd2-N6	2.478(4)	N7-Gd2-N9	107.63(15)

[a] Gd1–Ind means the average bond distances between the rare-earth metal ion and the five-membered heterocyclic ring of the indolyl ligand.

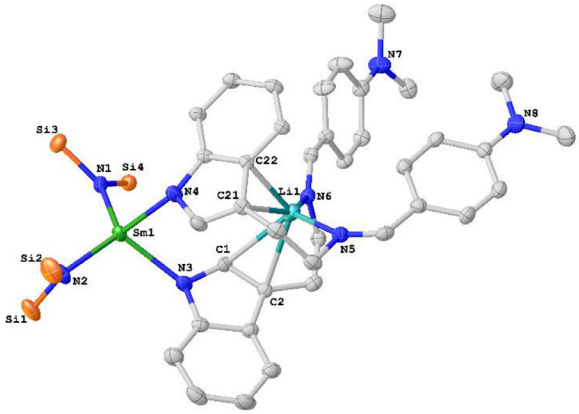

Fig. 4. Structure of complex **7**. Hydrogen atoms and the CH_3 of $N(SiMe_3)_2$ group were omitted for clarity.

C-N (intermediate **E)** bonds sequentially, leading to the formation of **6**.

When $[(Me_3Si)_2N]_3Sm(\mu\text{-Cl})Li(THF)_3$ was reacted with 2 equiv. of H**L** at 80 °C in toluene, the hetero-nuclear bimetallic bis(indolyl) rare-earth metal complex **7** $\{(\eta^1{:}\eta^1\text{-}[\mu\text{-}\eta^2{:}\eta^1\text{-}3\text{-}(4\text{-}Me_2N\text{-}C_6H_4CH{=}N\text{-}CH_2CH_2)C_8H_5]Li[\mu\text{-}\eta^2{:}\eta^1\text{-}3\text{-}(4\text{-}Me_2N\text{-}C_6H_4CH{=}NCH_2CH_2)C_8H_5])Sm[N(SiMe_3)_2]\}$ was obtained alone with complex **2** (Scheme 2, route c, Fig. 4).

The X-Ray diffraction studies revealed that the Sm^{3+} ion was ligated with two N atoms of two indolyl ligands and two $N(SiMe_3)_2$ groups, forming a four-coordinated anionic Sm^{3+} center. The Li^+ ion lies in a distorted tetrahedral geometry, consisting of two indolyl ring in an η^2 fashion and two pendant imino groups, where the coordination mode of indolyl ring is similar to those in complexes **1**-**5**. The Sm-$N_{indolyl}$ (2.349(6) and 2.382(6)Å) and Sm-N_{amido} (2.290(5)Å, 2.289(5)Å) bond lengths in **7** are comparable to those (Sm-$N_{indolyl}$ = 2.352(6)Å, Sm-N_{amido} = 2.283(6) and 2.265(5)Å) in complex **2**, and both are comparable to the reported hetero-nuclear bimetallic complexes $\{\eta^1{:}\eta^1\text{-}[\eta^1\text{-}3\text{-}(2\text{-}(N\text{-}CH_3)C_4H_3N\text{-}CH{=}NCH_2CH_2)C_8H_5N]Li[\mu\text{-}\eta^2{:}\eta^1\text{-}3\text{-}(2\text{-}(N\text{-}CH_3\text{-}C_4H_3N\text{-}CH{=}N\text{-}CH_2CH_2)\ C_8H_5N])RE[N(SiMe_3)_2]_2\}$ (RE = Yb, Dy) [2g], if the difference of their ionic radii were considered.

2.3. Spectroscopic analysis

It is well-known that the rare-earth-metal complexes play an important role in material chemistry, due to their distinctive and excellent luminescent performance. In order to explore the fluorescent properties of the complexes **1**-**5**, the UV-vis absorption and

Table 3
Selected bond lengths (Å) and angles (°) for complex **7**.

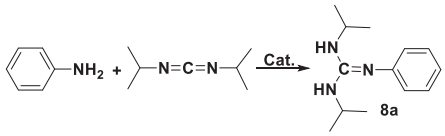

7	Bond length(Å)		Angles (°)
Sm-N1	2.290(5)	N1-Sm-N2	120.98(18)
Sm-N2	2.289(5)	N1-Sm-N3	112.68(18)
Sm-N3	2.349(6)	N1-Sm-N4	109.06(19)
Sm-N4	2.382(6)	N5-Li-N6	124.4(6)
Li-C1	2.830(14)	N5-Li-C1	131.0(6)
Li-C2	2.671(14)	N5-Li-C2	106.4(5)
Li-C21	2.562(13)	C1-Li-C2	28.4(2)
Li-C22	2.425(13)	C21-Li-C22	32.9(2)
Li-N5	2.064(13)	Cl-Li-C21	97.3(5)
Li-N6	2.051(12)	N6-Li-C21	154.6(6)

fluorescent properties of the complexes **1**-**5** were measured both in solution and in the solid state. The absorption and emission spectra of the ligand (HL) and the complexes **1**-**5** in acetonitrile are shown in Figures S59-60 (see the SI). The solid-state photoluminescence data for the complexes **1**-**5** are given in the figures S61-S65 (see the SI). Unfortunately, all the characteristic transitions for the RE^{3+} ions were not observed in the complexes **1**-**5**. The reason may be explained by the fact that the energy level of the ligand is not well matched with the rare-earth ions in the complexes, resulting in lower energy transfer efficiency [14].

2.4. Catalytic activities on addition of amines N–H bond to carbodiimides

The catalytic activities of the imino-functionalized indolyl ligand incorporating rare-earth metal amido complexes on amines addition to carbodiimides were examined (Table 4).

Complex **1** was used as catalyst for the model reaction of the aniline with *N, N'*-diisopropylcarbodiimide (DIC). The yields of the

Table 4
Optimization of the conditions on the catalytic addition of the aniline N-H bond to N, N'-diisopropylcarbodiimide (DIC).

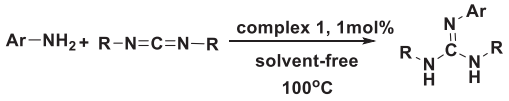

Entry[a]	Cat.(mol %)	Solv.	Temp. (°C)/Time (h)	Yield(%)[b]
1	**1**(0.5)	THF	r.t./12	71
2	**1**(1.0)	THF	r.t./12	83
3	**1**(2.0)	THF	r.t./12	85
4	**1**(1.0)	Hexane	r.t./12	79
5	**1**(1.0)	Toluene	r.t./12	84
6	**1**(1.0)	CH_2Cl_2	r.t./12	76
7	**1**(1.0)	Solvent-free	r.t./12	89
8	**1**(1.0)	Solvent-free	40/12	91
9	**1**(1.0)	Solvent-free	70/12	95
10	**1**(1.0)	Solvent-free	100/12	97
11	**1**(1.0)	Solvent-free	100/6	97
12	**1**(1.0)	Solvent-free	100/2	97
13	**2**(1.0)	Solvent-free	100/2	85
14	**3**(1.0)	Solvent-free	100/2	82
15	**4**(1.0)	Solvent-free	100/2	83
16	**5**(1.0)	Solvent-free	100/2	93
17	**6**(1.0)	Solvent-free	100/2	83
18	**7**(1.0)	Solvent-free	100/2	92

[a] Reaction conditions: diisopropylcarbodiimide (1.0 mmol), phenylamine (1.0 mmol), solvent (2 mL) or solvent-free.
[b] Isolated yields.

Table 5
Results of reactions of different amines with carbodiimides catalyzed by complex **1.**

Entry[a]	R	Ar	Product	Yield(%)[b]
1	^{i}Pr	C_6H_5	**8a**	97
2	Cy		**8b**	97
3	^{i}Pr	4-MeC_6H_4	**8c**	77
4	Cy		**8d**	78
5	^{i}Pr	2-MeC_6H_4	**8e**	76
6	Cy		**8f**	78
7	^{i}Pr	2-$OMeC_6H_4$	**8g**	80
8	Cy		**8h**	81
9	^{i}Pr	4-$OMeC_6H_4$	**8i**	78
10	Cy		**8j**	78
11	^{i}Pr	2-$^{t}BuC_6H_4$[c]	**8k**	40 [c]
12	Cy		**8l**	46 [c]
13	^{i}Pr	2,6-$Me_2C_6H_3$[c]	**8m**	55 [c]
14	Cy		**8n**	56 [c]
15	^{i}Pr	2-$NO_2C_6H_4$	**8o**	82
16	Cy		**8p**	85
17	^{i}Pr	4-$NO_2C_6H_4$	**8q**	83
18	Cy		**8r**	86
19	^{i}Pr	4-BrC_6H_4	**8s**	93
20	Cy		**8t**	93
21	^{i}Pr	4-ClC_6H_4	**8u**	80
22	Cy		**8v**	81

[a] Reaction conditions: carbodiimide (1.0 mmol), aromatic amine (1.0 mmol), catalyst loading (1 mol %), solvent-free, 100 °C, reaction time 2 h.
[b] Isolated yields.
[c] Reaction time 12 h.

catalytic guanylation reaction were raised along with an increase of catalyst loading (Table 4, entries 1-3), but while the loading of catalyst **1** was increased from 1 mol% to 2 mol%, the yield of guanidine **8a** was raised slowly (Table 4, entries 2-3). It is indicated that the effect on the reaction became less and less with the increase of catalyst loading. The reaction was carried out under different solvent conditions with 1mol % catalyst loading, toluene seemed to be a better solvent than other solvents (THF, hexane or CH_2Cl_2) for the reaction (Table 4, entries 3-6). Many previous works reported that rare-earth metal complexes have excellent performance in the guanylation reaction under solvent-free condition [10c-f]. On account of this, complex **1** on the addition reaction of aniline to DIC was tested under solvent-free condition. The yield of the guanidine under solvent-free condition was the best one than under other solvents (Table 4, entry 7). Subsequent screening of reaction temperature based on the complex **1** indicated that 100 °C was optimal (Table 4, entries 8-10). When shorten the reaction time from 12 h to 2 h, a 97% yield of product could be obtained (Table 4, entry 12). The guanidine **8a** was obtained in 85%, 82%, 83%, 93%, 83% and 92% yields using the catalysts **2-6, 7** in 2 h (Table 4, entries 13-18) respectively, indicating that the central metal ions of the complexes had little influence on the catalytic activity. As a result, the reaction should perform better in the presence of 1 mol % complex **1** at 100 °C for 2 h under solvent-free conditions.

Next, different substrates of arylamines were tested under the above optimized conditions (Table 5).

As shown in Table 5, the complex **1** displays a good catalytic activity on guanylation reaction under solvent-free condition. The substituents on phenyl ring of the arylamines can be electron-withdrawing groups such as O_2N, Br, Cl or electron-donating groups such as CH_3O, CH_3. The reactions of amines with electron-withdrawing substituted groups (Table 5, entries 15-22) afford much more better results than those of amines with electron-donating substituted groups with carbodiimides (Table 5, entries 3-10). However, the reaction with a steric bulky amine, such as 2, 6-dimethylaniline or 2-tert-butylaniline, proceeded slowly and gave the corresponding guanidine in 40-56% yield, even prolonged reaction period to 12 h (Table 5, entries 11-14), maybe due to the steric hindrance. The result was also consistent with the previous reported works [9].

3. Conclusions

In summary, the reaction of rare-earth metal amides $[(Me_3Si)_2N]_3RE(\mu\text{-}Cl)Li(THF)_3$ with the imino-functionalized indolyl ligand (H**L**) under different reaction conditions generated three kinds of novel rare-earth metal amido complexes, including heteronuclear bimetallic monoindolyl complexes **1**-**5**, homonuclear bimetallic bis(indolyl) complex **6** and heteronuclear bimetallic bis(indolyl) complex **7**. The results indicated that the imino-functionalized indolyl ligand had multiple reactivity with rare-earth metal amides and diverse coordination modes with rare-earth metal ions. The catalytic activity of complexes **1**-**7** in the guanylation reaction was evaluated. All the complexes showed good activity towards the addition of amine to carbodiimides under solvent-free condition. Moreover, these complexes exhibited a good catalytic efficiency on the substituted arylamines with electron-withdrawing or small steric hindrance group on the phenyl rings. Further studies on the coordination chemistry and potential catalytic applications of the rare-earth metal complexes incorporating imino-functionalized indolyl ligand are still in progress.

4. Experimental

4.1. Materials and procedures

All syntheses and manipulations of air- and moisture-sensitive materials were performed under dry argon and an oxygen-free atmosphere using standard Schlenk techniques or in a glovebox. All solvents were refluxed and distilled over sodium benzophenone ketyl under argon prior to use unless otherwise noted. Other reagents were used in their commercial form without further purification. $[(Me_3Si)_2N]_3RE(\mu\text{-}Cl)Li(THF)_3$(RE = Y, Sm, Gd, Er, Yb) were prepared according to literature methods [15]. Elemental analyses were performed on a Perkin-Elmer 2400 CHN analyzer. Melting points were determined in sealed capillaries without correction. ^{1}H NMR and ^{13}C NMR spectra for analyses of compounds were recorded on a Bruker AV-500 NMR spectrometer (500 MHz for ^{1}H; 125 MHz for ^{13}C) in $CDCl_3$ or C_6D_6 or DMSO-d_6 for complexes. Chemical shifts (δ) were reported in ppm. J values are reported in Hz. HRMS was performed on a Waters VEVO G2 Q-TOF. The UV-vis absorption spectra were recorded on a UV-5900 PC. The luminescence spectra were recorded on FL-4600 Spectrophotometer. IR spectra were recorded on Nicolet-470 spectrometer (KBr pellet).

4.3. Synthesis of ligand and complexes

4.3.1. Synthesis of 3-(4-Me_2N-C_6H_4CH=N-CH_2CH_2)C_8H_5NH (H**L**)

A 100 mL round bottom flask with a magnetic stirrer bar was charged with (*N, N*-dimethylamino)benzaldehyde (1.492 g, 10.0 mmol) and tryptamine (1.602 g, 10.0 mmol), to which was added ethanol. The reaction mixture was stirred at room temperature for 4 h and during which time a yellow precipitate formed. And was filtered with suction to obtain a crude product, which was recrystallized from anhydrous methanol to obtain pale yellow crystals. The final product is obtained as yellow crystals (2.4153 g, 83% yield). mp: 144.9 °C. ^{1}H NMR (500 MH_Z, DMSO-d_6, 25 °C): δ 10.66 (s, 1H, N*H*), 7.98 (s, 1H, C*H*=N), 7.52 (d, J = 7.90 Hz, 1H, Ar*H*), 7.48 (d, J = 8.60 Hz, 2H, Ar*H*), 7.30 (t, J = 8.10 Hz, 1H, Ar*H*), 7.02 (t, J = 7.50 Hz, 2H, Ar*H*), 6.93 (t, J = 7.40 Hz, 1H, Ar*H*), 6.65 (d, J = 8.70 Hz, 2H, Ar*H*), 3.70 (t, J = 7.30 Hz, 2H, CH_2), 2.95 (t, J = 7.30 Hz, 2H, CH_2), 2.88 (s,

6H, N(CH_3)$_2$). ^{13}C NMR (125 MHz, $CDCl_3$):δ 161.8 (*C*=N), 152.4 (C_8H_5N), 136.7 (C_8H_5N), 129.9 (2 C_8H_5N), 128.0 (C_8H_5N), 124.8 (C_8H_5N),122.6 (C_8H_5N), 122.2 (C_8H_5N), 119.5 (C_8H_5N), 119.4 (C_6H_4), 114.6 (C_6H_4), 112.1 (C_6H_4), 111.5 (C_6H_4), 62.4 (CH_2), 41.3 (CH_3), 40.6 (CH_3), 27.6 (CH_2). IR (KBr pellets, cm^{-1}): ν3423(m), 3092(m, C_8H_5N-H), 2918(m), 2861(m), 1636(m), 1608(s, C=N), 1556(m), 1534(m), 1431(m), 1370(m), 1344(m), 1310(m), 1228(m), 1181(m), 807(m), 730(m). Anal. Calcd for $C_{19}H_{21}N_3$: C, 78.32; H, 7.26; N, 14.42; Found: C, 78.28; H, 7.25; N, 14.44.

*4.3.2. Synthesis of {[η^1:μ-η^2-3-(4-Me_2N-C_6H_4CH= N-CH_2CH_2)C_8H_5]Y[N($SiMe_3$)$_2$](μ-Cl)Li(THF)} (**1**)*

To a toluene (10.0 mL) solution of [(Me_3Si)$_2$N]$_3$Y(μ-Cl)Li(THF)$_3$(0.8288 g, 1 mmol) was added 3-(4-Me_2N-C_6H_4CH=N-CH_2CH_2)C_8H_5NH (0.2910 g, 1 mmol) under 1:1 ratio. After the solution was heated to 80 °C for 24 h, the color of the solution gradually changed to yellow. The solvent was evaporated under reduced pressure. The residue was extracted with hexane. Colorless crystals were obtained at room temperature after several days (0.2849 g, 35% yield). mp:186 °C. ^{1}H NMR (500 MHz, C_6D_6, 25 °C): δ 8.40 (d, *J* = 8.25 Hz, 1H, C*H*=N), 8.00 (s, 1H, Ar*H*), 7.68 (s, 1H, Ar*H*), 7.48-7.53 (m, 3H, Ar*H*), 7.33-7.36 (m, 1H, Ar*H*), 7.14-7.16 (m, 1H, Ar*H*), 6.40 (d, *J* = 8.95 Hz, 2H, Ar*H*), 3.54 (t, *J* = 10.85 Hz, 2H, C_4H_8O), 2.85 (t, *J* = 11.35 Hz, 2H, C_4H_8O), 2.69 (s, 4H, C_4H_8O), 2.20 (s, 6H, -N(CH_3)$_2$), 0.87 (t, *J* = 11.75 Hz, 4H, CH_2), 0.57 (m, 36H, Si(CH_3)$_3$).^{13}C NMR (125 MHz, C_6D_6, 25 °C): δ 165.8 (*C*H=N), 152.8 (C_8H_5N), 146.4 (C_8H_5N), 131.1 (C_8H_5N),130.5 (C_8H_5N), 130.2 (C_8H_5N), 122.1 (C_8H_5N), 121.3 (C_8H_5N), 119.8 (C_8H_5N), 118.4 (C_6H_4), 118.0 (C_6H_4), 111.8 (C_6H_4), 111.2 (C_6H_4), 67.8 (C_4H_8O), 61.6 (C_4H_8O), 39.6 (C_4H_8O), 39.3 (C_4H_8O), 27.5 (CH_2), 24.9 (CH_2), 5.6 (CH_3), 5.5 (CH_3), 5.2 (CH_3). IR (KBr pellets, cm^{-1}): ν 3423 (s), 2917 (m), 2861 (m), 1637 (m), 1607 (s, -C=N-), 1556 (m), 1533 (m), 1443 (m), 1431 (m), 1370 (m), 1344 (m), 1310 (m), 1228 (m), 1181 (m), 1111 (m), 1073 (m), 1044 (m), 807 (m), 730 (m), 595 (m), 523 (m), 489 (m), 424 (m). Anal. Calcd for $C_{35}H_{64}ClLiN_5OSi_4Y$: C, 51.51; H, 7.92; N, 8.60; Found: C, 51.71; H, 7.61; N, 8.83.

*4.3.3. Synthesis of {[η^1:μ-η^2-3-(4-Me_2N-C_6H_4CH= N-CH_2CH_2)C_8H_5]Sm[N($SiMe_3$)$_2$](μ-Cl)Li(THF)} (**2**)*

The complex **2** following a procedure similar to that described for the preparation of complex **1** by reaction of HL (0.2910 g, 1 mmol) with [(Me_3Si)$_2$N]$_3$Sm(μ-Cl)Li(THF)$_3$ (0.890 g, 1 mmol) in toluene (10.0 mL) at 80 °C for 24 h in a 1:1 ratio. Colorless crystals were obtained at room temperature after several days from hexane solution (0.2251 g, 25%). mp: 191.1°C;^{1}H NMR (500 MHz, C_6D_6): δ 14.77 (d, *J* = 6.6 Hz, 1H, C*H*=N), 12.55 (s, 1H, Ar*H*), 8.97 (d, *J* = 6.5 Hz, 1H,Ar*H*), 8.56 (d, *J* = 7.6 Hz, 1H, Ar*H*), 8.48 (s, 1H, Ar*H*), 8.14 (t, *J* = 7.2 Hz, 1H, Ar*H*), 8.09 (d, J = 8.9 Hz, 2H, Ar*H*), 6.27 (d, *J* = 9.0 Hz, 2H, Ar*H*), 4.76 (m, 2H, C_4H_8O), 3.82-3.74 (m, 2H, C_4H_8O), 3.53 (s, 4H, C_4H_8O), 2.04 (s, 6H, N(CH_3)$_2$), -1.24 (s, 4H, CH_2), -1.49 (s, 36H, (Si(CH_3)$_3$). ^{13}C NMR (125 MHz, C_6D_6): δ 166.9 (*C*H=N), 152.9 (C_8H_5N), 130.9 (C_8H_5N), 123.6 (C_8H_5N), 122.8 (C_8H_5N), 120.3 (C_8H_5N), 119.4 (C_6H_4), 111.9 (C_6H_4), 68.6 (C_4H_8O), 62.8 (C_4H_8O), 39.8 (C_4H_8O), 39.2 (C_4H_8O), 29.1 (CH_2), 25.4 (CH_2), 3.5 (CH_3), 3.0 (CH_3), 2.7 (CH_3). IR (KBr pellets, cm^{-1}): ν 3397(m), 2975(m), 2899(m), 1637(m), 1607(s, C=N), 1556(m), 1533(m), 1444(m), 1431(m), 1371(m), 1344(m), 1310(m), 1234(m), 1181(m), 1088(m), 1047(m), 880(m), 806(m), 729(m), 609(m), 500(m). Anal. Calcd for $C_{35}H_{64}ClLiN_5OSi_4Sm$: C, 47.99; H, 7.36; N, 7.99; Found:C, 47.26; H, 7.26; N, 7.73.

*4.3.4. Synthesis of {[η^1:μ-η^2-3-(4-Me_2N-C_6H_4CH= N-CH_2CH_2)C_8H_5]Gd[N($SiMe_3$)$_2$](μ-Cl)Li(THF)} (**3**)*

The complex **3** following a procedure similar to that described for the preparation of complex **1** by reaction of HL (0.2910 g, 1 mmol) with [(Me_3Si)$_2$N]$_3$Gd(μ-Cl)Li(THF)$_3$ (0.8973 g, 1 mmol) in toluene (10.0 mL) at 80 °C for 24 h in a 1:1 ratio. Colorless crystals were obtained at room temperature after several days from hexane solution (0.2042 g, 23%). mp: 189.9°C. IR (KBr pellets, cm^{-1}): ν 3442(m), 2960(m), 2861(m), 1637(m), 1607(s, -C=N-), 1556(m), 1533(m), 1443(m), 1431(m), 1370(m), 1344(m), 1309(m), 1260(m), 1227(m), 1181(m), 1109(m), 1070(m), 1043(m),1022(m), 842(m), 806(m), 729(m), 568(m), 524(m), 489(m), 419(m). Anal. Calcd for $C_{35}H_{64}ClLiN_5OSi_4Gd$: C, 47.61; H, 7.31; N, 7.93; Found: C, 47.03; H, 7.25; N, 7.70.

*4.3.5. Synthesis of {[η^1:μ-η^2-3-(4-Me_2N-C_6H_4CH= N-CH_2CH_2)C_8H_5]Er[N($SiMe_3$)$_2$](μ-Cl)Li(THF)} (**4**)*

The complex **4** following a procedure similar to that described for the preparation of complex **1** by reaction of HL (0.2910 g, 1 mmol) with [(Me_3Si)$_2$N]$_3$Er(μ-Cl)Li(THF)$_3$ (0.9080 g, 1 mmol) in toluene (10.0 mL) at 80°C for 24 h in a 1:1 ratio. Pink crystals were obtained at room temperature after several days from hexane solution (0.2697g, 30%). mp: 188.3°C. IR (KBr pellets, cm^{-1}): ν 3443(m), 2918(m), 2861(m), 1636(m), 1608(s, -C=N-), 1556(m), 1533(m), 1444(m), 1431(m), 1370(m), 1344(m), 1310(m) 1227(m), 1181(m), 1111(m), 1044(m), 807(m), 730(m), 608(m), 524(m), 489(m), 424(m). Anal. Calcd for $C_{35}H_{64}ClLiN_5OSi_4Er$: C, 47.08; H, 7.22; N, 7.84; Found:C, 46.95; H, 7.21; N, 7.94.

*4.3.6. Synthesis of {[η^1:μ-η^2-3-(4-Me_2N-C_6H_4CH= N-CH_2CH_2)C_8H_5]Yb[N($SiMe_3$)$_2$](μ-Cl)Li(THF)} (**5**)*

The complex **5** following a procedure similar to that described for the preparation of complex **1** by reaction of HL (0.2910 g, 1 mmol) with [(Me_3Si)$_2$N]$_3$Yb(μ-Cl)Li(THF)$_3$ (0.9129 g, 1 mmol) in toluene (10.0 mL) at 80 °C for 24 h in a 1:1 ratio. Yellow crystals were obtained at room temperature after several days from hexane solution (0.3685g, 41% yield). mp: 191 °C. IR (KBr pellets, cm^{-1}): ν 3422(m), 2917(m), 2858(m), 1637(m), 1607(s, -C=N-,), 1555(m), 1532(m), 1443(m), 1431(m), 1369(m), 1310(m), 1228(m), 1180(m), 807(m), 730(m), 608(m), 525(m), 499(m), 423(m). Anal.Calcd for $C_{35}H_{64}ClLiN_5OSi_4Yb$: C, 46.78; H, 7.18; N, 7.79; Found: C, 46.28; H, 7.29; N, 7.62.

*4.3.7. Synthesis of {[(μ-η^5:η^1):η^1:η^1-3-[(Me_2N)$_2C_{14}H_9$](N$CH_2CH_2C_8H_5N$)$_2$]Gd_2[N(Si-Me_3)$_2$]$_3$} (**6**)*

To a toluene (10.0 mL) solution of [(Me_3Si)$_2$N]$_3$Gd(μ-Cl)Li(THF)$_3$(0.8973 g, 1 mmol) was added 3-(4-Me_2N-C_6H_4CH=N-CH_2CH_2)C_8H_5NH (0.2910 g, 1 mmol) in a 1:1 ratio. After the reaction mixture was heated to 80 °C for 72 h and the color of the solution gradually changed to yellow. The solvent was evaporated under reduced pressure. The residue was extracted with hexane. Yellow crystals were obtained at room temperature after several days (0.1653 g, 12% yield). mp: 233 °C. IR (KBr pellets, cm^{-1}): ν 3416(m), 3127(m), 3092(m), 3006(m), 2917(m), 2861(m), 1637(m), 1607(s, -C=N-), 1556(m), 1533(m), 1431(m), 1370(m), 1344(m), 1181(m), 807(m), 730(m). Anal. Calcd for $C_{56}H_{93}Gd_2N_9Si_6$: C, 48.90; H, 6.82; N, 9.17; Found: C, 51.38; H, 5.86; N, 8.90.

*4.3.8. Synthesis of {(η^1:η^1-[μ-η^2:η^1-3-(4-Me_2N-C_6H_4CH= N-CH_2CH_2)C_8H_5]Li-[μ-η^2:η^1-3-(4-Me_2N-C_6H_4CH= N-CH_2CH_2)C_8H_5])Sm[N($SiMe_3$)$_2$]} (**7**)*

To a toluene (10.0 mL) solution of [(Me_3Si)$_2$N]$_3$Sm(μ-Cl)Li(THF)$_3$ (0.890 g, 1 mmol) was added 3-(4-Me_2N-C_6H_4CH=N-CH_2CH_2)C_8H_5NH (0.5820 g, 2 mmol) in a 1:2 ratio. After the reaction mixture was heated to 80 °C for 48 h, the color of the solution gradually changed to yellow. The solvent was evaporated under reduced pressure. The residue was extracted with hexane. Yellow crystals were obtained at room temperature after several days (0.2214 g, 25% yield). mp: 160 °C. IR (KBr pellets, cm^{-1}): ν 3414(m), 2916(m), 2848(m), 1636(m), 1604(s, -C=N-), 1527(m), 1482(m), 1456(m), 1361(m), 1312(m), 1259(m), 1179(m), 1097(m), 944(m), 816(m), 742(m), 594(m), 405(m).

4.4. General experimental procedure for synthesis of guanidines (product **8a** as an example)

A 30 mL Schlenk tube under dried argon was charged with the complex **1**. To the flask were added *N, N′*-diisopropylcarbodiimide (0.1263 g, 1 mmol), and aniline (0.0931 g, 1 mmol). The resulting mixture was stirred at 100 °C for 2 h. Then, the reaction mixture was hydrolyzed with water (1 mL) and extracted with dichloromethane (3 × 10 mL), and the extracts were dried over anhydrous Na_2SO_4 and filtered. After the solvent was removed under reduced pressure. The final product could be obtained by hexane afford crystalline. The detailed ^1H and $^{13}C\{^1H\}$ NMR spectra of compounds **8a**-**8v** are included in the SI.

4.5. X-ray crystallographic study

A suitable crystal of complexes **1**-**5, 6** and **7** was each mounted in a sealed capillary. Diffraction was performed on a Bruker SMART APEX II CCD area detector diffractometer using graphite-monochromated Mo-Kα radiation (λ = 0.71073 Å), temperature 293(2) K for **1**-**3** and **7**, and 273(2) K for **4**-**5**, and 298(2) K for **6**, with φ and ω scan technique. An empirical absorption correction was applied using the SADABS program. All structures were solved by direct methods, completed by subsequent difference Fourier syntheses, and refined anisotropically for all non-hydrogen atoms by full-matrix least-squares calculations based on F^2 using the SHELXTL programpackage. The hydrogen atom coordinates were calculated with SHELXTL by using an appropriate riding model with varied thermal parameters. The residual electron densities were of no chemical significance. Selected bond lengths and angles are compiled in Tables 1–3, and crystal data and details of the data collection and structure refinements are given in Support Information. CCDC 2010885-2010891 contains the supplementary crystallographic data for complexes **1**-**5, 6** and **7**, respectively. These data can be obtained free of charge from The Cambridge Crystallographic Data Centre via www.ccdc.cam.ac.uk/data_request/cif.

Declaration of Competing Interest

The authors declare that they have no known competing financial interests or personal relationships that could have appeared to influence the work reported in this paper.

Acknowledgements

This work was supported by the National Natural Science Foundation of China (grant No. 21602157), Anhui Provincial Natural Science Foundation (grant No. 1908085QB50), Anhui Laboratory of Molecule-Based Material (grant No. fzj19015), The Excellent Young Talents Fund Program of Higher Education Institutions of Anhui Province (grant No. gxyq2019041).

Supplementary materials

Supplementary material associated with this article can be found, in the online version, at doi:10.1016/j.jorganchem.2020.121661.

References

[1] (a) Y. Shimazaki, T. Yajimab, M. Takani, O. Yamauchi, Coord. Chem. Rev. 253 (2009) 479; (b) T. Matsugi, S. Matsui, S.-i. Kojoh, Y. Takagi, Y. Inoue, T. Nakano, T. Fujita, N. Kashiwa, Macromolecules 35 (2002) 4880–4887; (c) Y. Yang, Q. Wang, D. Cui, J. Polym. Sci., Part A 46 (2008) 5251–5262.

[2] (a) X. Zhu, S. Zhou, S. Wang, Y. Wei, L. Zhang, F. Wang, S. Wang, Z. Feng, Chem. Commun. 48 (2012) 12020–12022; (b) X. Zhu, S. Wang, S. Zhou, Y. Wei, L. Zhang, F. Wang, Z. Feng, L. Guo, X. Mu, Inorg. Chem. 51 (2012) 7134–7143; (c) G. Zhang, Y. Wei, L. Guo, X. Zhu, S. Wang, S. Zhou, X. Mu, Chem. Eur. J. 21 (2015) 2519–2526; (d) G. Zhang, B. Deng, S. Wang, Y. Wei, S. Zhou, X. Zhu, Z. Huang, X. Mu, Dalton Trans. 45 (2016) 15445–15456; (e) Z. Feng, Y. Wei, S. Zhou, G. Zhang, X. Zhu, L. Guo, S. Wang, X. Mu, Dalton Trans. 44 (2015) 20502–20513; (f) S. Yang, X. Zhu, S. Zhou, S. Wang, Z. Feng, Y. Wei, H. Miao, L. Guo, F. Wang, G. Zhang, X. Gu, X. Mu, Dalton Trans. 43 (2014) 2521–2533; (g) S. Yang, X. Zhu, S. Zhou, et al., Sci China Chem 57 (8) (2014) 1090–1097; (h) L. Guo, X. Zhu, G. Zhang, Y. Wei, L. Ning, S. Zhou, Z. Feng, S. Wang, X. Mu, J. Chen, Y. Jiang, Inorg. Chem. 54 (2015) 5725–5731; (i) G. Zhang, S. Wang, S. Zhou, Y. Wei, L. Guo, X. Zhu, L. Zhang, X. Gu, X. Mu, Organometallics 34 (17) (2015) 4251–4261; (j) X. Zhu, Y. Li, Y. Wei, S. Wang, S. Zhou, L. Zhang, Organometallics 35 (2016) 1838–1846; (k) X. Zhu, Y. Jiang, J. Chen, S. Wang, Z. Huang, S. Zhu, X. Zhao, W. Yue, J. Zhang, W. Wu, X. Zhong, Chin. J. Chem. 38 (2020) 478–488.

[3] (a) R.G.S. Berlinck, Nat. Prod. Rep. 13 (1996) 377–409; (b) R.G.S. Berlinck, A.C.B. Burtoloso, E.T.-S. Amaro, S. Romminger, R.P. Morais, K. Bandeira, C.M. Mizuno, Nat. Prod. Rep. 27 (2010) 1871–1907; (c) S. Tahir, A. Badshah, R.A. Hussain, Bioorg. Chem. 59 (2015) 39–79.

[4] (a) R. Kuppusamy, M. Yasir, E. Yee, M. Willcox, D. StC. Black, N. Kumar, Org. Biomol. Chem. 16 (2018) 5871–5888; (b) Y.-C. Lin, A. Ribaucourt, Y. Moazami, J.G. Pierce, J. Am. Chem. Soc. 142 (2020) 9850–9857.

[5] (a) V. Previtali, C. Trujillo, R. Amet, D.M. Zisterer, I. Rozas, Med. Chem. Commun. 9 (2018) 735–743; (b) M. Staszewski, A. Stasiak, T. Karcz, D. McN. Flores, W.A. Fogel, K. Kieć-Kononowicz, R. Leurs, K. Walczyński, Med. Chem. Commun. 10 (2019) 234–251; (c) R. Blaszczyk, J. Brzezinska, B. Dymek, P.S. Stanczak, M. Mazurkiewicz, J. Olczak, J. Nowicka, K. Dzwonek, A. Zagozdzon, J. Golab, A. Golebiowski, ACS Med. Chem. Lett. 11 (4) (2020) 433–438.

[6] (a) M.P. Coles, Dalton Trans. 35 (2006) 985–1001; (b) N. Liu, B. Liu, D. Cui, Dalton Trans. 47 (2018) 12623–12632; (c) Q. Chen, L. Xie, Z. Li, Y. Tang, P. Zhao, L. Lin, X. Feng, X. Liu, Chem. Commun. 54 (2018) 678–681; (d) J. Francos, V. Cadierno, Dalton Trans., 48 (2019) 9021–9036; (e) T. Peddarao, N. Sarkar, S. Nembenna, Inorg. Chem. 59 (7) (2020) 4693–4702.

[7] (a) F.T. Edelmann, Chem. Soc. Rev. 38 (2009) 2253–2268; (b) F.T. Edelmann, Chem. Soc. Rev. 41 (2012) 7657–7672; (c) T. Zeng, Q. Qian, B. Zhao, D. Yuan, Y. Yao, Q. Shen, RSC Adv., 5 (2015) 53161–53171; (d) F. Kong, M. Li, X. Zhou, L. Zhang, RSC Adv., 7 (2017) 29752–29761.

[8] (a) G. Vaidyanathan, M.R. Zalutsky, J. Org. Chem. 62 (1997) 4867–4869; (b) M.K.T. Tin, N. Thirupathi, G.P.A. Yap, D.S. Richeson, Dalton Trans. 17 (1999) 2947–2950; (c) Y.Q Wu, S.K. Hamilton, D.E. Wilkinson, G.S. Hamilton, J. Org. Chem. 67 (2002) 7553–7556; (d) A. Turočkin, R. Honeker, W. Raven, P. Selig, J. Org. Chem. 81 (2016) 4516–4529.

[9] (a) T.G. Ong, G.P.A. Yap, D.S. Richeson, J. Am. Chem. Soc. 125 (2003) 8100–8101; (b) C. Alonso-Moreno, A. Antiñolo, F. Carrillo-Hermosilla, A. Otero, Chem. Soc. Rev. 43 (2014) 3406–3425; (c) A. Baishya, M. Kr. Barman, T. Peddarao, S. Nembenna, J. Organomet. Chem. 769 (2014) 112–118; (d) W. Zhang, L. Xu, Z. Xi, Chem. Commun. 51 (2015) 254–265.

[10] (a) W. Zhang, M. Nishiura, Z. Hou, Chem. Eur. J. 13 (2007) 4037–4051; (b) Q. Li, S. Wang, S. Zhou, G. Yang, X. Zhu, Y. Liu, J. Org. Chem. 72 (2007) 6763–6767; (c) X. Zhu, Z. Du, F. Xu, Q. Shen, J. Org. Chem. 74 (2009) 6347–6349; (d) R. Jiao, M. Xue, X. Shen, Y. Zhang, Y. Yao, Q. Shen, Eur. J. Inorg. Chem. (2010) 2523–2529; (e) Z. Li, M. Xue, H. Yao, H. Sun, Y. Zhang, Q. Shen, J. Organomet. Chem. 713 (2012) 27–34; (f) L. Cai, Y. Yao, M. Xue, Y. Zhang, Q. Shen, Appl. Organomet. Chem. 27 (2013) 366–372; (g) H. Cheng, Y. Xiao, C. Lu, B. Zhao, Y. Wang, Y. Yao, New J. Chem. 39 (2015) 7667–7671; (h) C. Lu, C. Gong, B. Zhao, L. Hu, Y. Yao, J. Org. Chem. 83 (2018) 1154–1159.

[11] (a) G. Song, W.N.O. W., Z. Hou, J. Am. Chem. Soc. 136 (2014) 12209–12212; (b) H. Nagae, Y. Shibata, H. Tsurugi, K. Mashima, J. Am. Chem. Soc. 137 (2015) 640–643; (c) B. Guan, B. Wang, M. Nishiura, Z. Hou, Angew. Chem., Int. Ed. 52 (2013) 4418–4421; (d) G. Song, W. Li, M. Nishiura, Z. Hou, Chem. Eur. J. 21 (2015) 8394–8398.

[12] (a) P.L. Diaconescu, Acc. Chem. Res. 43 (2010) 1352–1363; (b) S.-J. Lou, Z. Mo, M. Nishiura, Z. Hou, J. Am. Chem. Soc. 142 (2020) 1200–1205.

[13] X. Cong, G. Zhan, Z. Mo, M. Nishiura, Z. Hou, J. Am. Chem. Soc. 142 (2020) 5531–5537.

[14] J.-L. Du, X.-Y. Wang, X.-Y. Zou, Y.-X. Li, W.-Z. Li, X. Yao, G.-M. Li, Luminescence 33 (2018) 1040–1047.

[15] (a) S. Zhou, S. Wang, G. Yang, X. Liu, E. Sheng, K. Zhang, L. Cheng, Z. Huang, Polyhedron 22 (2003) 1019–1024; (b) E. Sheng, S. Wang, G. Yang, S. Zhou, K. Zhang, L. Cheng, Z. Huang, Organometallics 22 (2003) 684–692.